Analysis of the stability and the consumption of an electrodynamic bearing for different operation conditions

Virginie Kluyskens*
Universite Catholique de Louvain
Center for Research in Mechatronics (CEREM)

Bruno Dehez
Universite Catholique de Louvain
Center for Research in Mechatronics (CEREM)

Abstract

In centering electrodynamic bearings, the guiding forces result from the interaction between eddy currents generated by a magnetic flux variation in conductors and the magnetic field. Predicting the dynamical behavior of this kind of bearings is not easy given the interactions between the electromagnetic nature of the forces and the rotational machinery aspects. In this paper, an electromechanical model, able to explain, predict, analyze and simulate the dynamical behavior of bearings submitted to eddy current forces, is applied on a homopolar null-flux electrodynamic bearing. The identification of the model's parameters is done based on quasi-static FEM simulation results. Thanks to the insight the electromechanical model gives on the physics involved in the bearing, the dynamical stability and the stiffness of the bearing are analyzed as a function of the bearing spin speed. For various operation conditions like a constant external load or a static unbalance, the behavior of the electrodynamic bearing is simulated and examined using the electromechanical model. For all these operation conditions, the influence of the external damping, necessary to stabilize the system is analyzed. The amount of necessary damping to introduce is discussed and also its impact on the overall bearing consumption.

1 Introduction

Magnetic bearings can be classified in different categories, as explained in [1], for instance as being active or passive. Active magnetic bearings use control systems to command the electromagnetic forces. Most common active magnetic bearings utilize an electromagnet in which the current intensity is controlled. In opposition to those active magnetic bearings, passive magnetic bearings do not use control systems. This implies that their characteristics can not be modulated, and the stiffness they generate is usually lower than in active magnetic bearings. However, they are usually simpler to use, cheaper, have a lower power consumption, and are intrinsically more reliable. However, passive magnetic bearings based only on permanent magnet interactions or reluctance forces can not be stable, according to the Earnshaw theorem [2]. They are then combined with other kind of bearings for the remaining degrees of freedom, in order to achieve stability. For instance, they may be combined with other kinds of passive magnetic bearings, which are not submitted to the Earnshaw theorem, like diamagnetic bearings, superconducting bearings, permanent magnet bearings stabilized by a gyroscopic torque, or electrodynamic bearings. In electrodynamic bearings, eddy current forces are intentionnaly generated to create the necessary centering forces. Electrodynamic bearings have the advantages to be passive and cheap. Moreover, null flux electrodynamic bearings do not generate forces, and thus no losses, unless needed, when the rotor is out-centered for instance. Examples of particular electrodynamic bearings can be found in [3] and [4]. However, electrodynamic bearings are not easy to design, and the stiffness they produce depends on the spin speed of the rotor. Modeling the forces due to the eddy currents adequately in dynamic conditions is important, in order to be able to simulate the dynamical behavior of the bearing and to predict its performances. But this study is not easy because two aspects have to be taken into account: the electromagnetic nature of the forces, and the rotor dynamic aspects, and the interactions between these two aspects.

Modeling the dynamical behavior of a magnetic bearing, including the mechanic and electric dynamics of the bearing, with finite elements is very heavy, and is not possible to realize reasonably nowadays. Furthermore, finite elements model do not offer any insight on the physics involved nor on the parameters influencing the bearing behavior. Analytical models have already been developed for particular electrodynamic bearings [4],[5]. In each case, the particular model of the proposed magnetic bearing structure is then used to determine the necessary damping and to predict the dynamical behavior of the bearing. These models were developed by solving the Maxwell's equations, and when the topology of the bearing is changed, the whole process needs to be done again. Furthermore, in both models restrictive hypothesis are made in order to be able to solve the Maxwell's equations, or even in order to be able to study the rotor dynamic stability. Besides, such a model does not allow a comprehensive understanding of all the physical principles involved and interactions, nor an easy analyze of the parameters influence, nor to be used to draw general conclusions on magnetic bearings development. This shows the need

*Contact Author Information: virginie.kluyskens@uclouvain.be, Place du Levant, 2, bte L5.04.02, 1348 Louvain-la-Neuve, Belgium, +32/10.47.22.83

for a general comprehensive electromechanical model able to predict the dynamical behavior of such bearings. In [6] and in [7], a general parameterized electromechanical model is described. The model is based on a direct analogy between the resistive-inductive dynamics of eddy currents and the spring-damper in series dynamics. The model focuses on the dynamical behavior of purely electrodynamic magnetic radial and thrust bearings [6], for homopolar and heteropolar bearings [7]. Stability is examined for a Jeffcott rotor on these kind of bearings. It is shown, based on a root loci study, that the rotor is wholeheartedly unstable when used alone: external non rotating damping is necessary to stabilize the system. Solutions are proposed in [8].
The model used in the present paper is presented in [9], [10] and [11]. For this model, a macroscopic point of view is chosen as to the electromagnetic phenomena involved in the system. This allows us to generalize the model to all kind of radial magnetic bearing subject to eddy currents. These bearings are modeled by mechanical components, like springs, for reluctant forces, and dampers, for eddy current forces [9] and [10]. The choice of the way to introduce these mechanical components in the electromechanical model is the result of a rigorous approach based on the electrical and the mechanical power present in the system, [11]. With this parameterized model, there is no need to develop an often complex analytical solution for the electric and the magnetic fields. The resistive and the inductive behavior of the eddy currents is also taken into account, and an analysis is made of the skin effect on this behavior at high rotating spin speed [12].
The parameters of the electromechanical system can be identified by forces measurements at different spin speed either through finite element simulations or through experiments, as explained in [11].
The developed electromechanical system shows the existence of an unstable spin speed range, or in other words the existence of two limit spin speeds between which the system behaves unstable in the radial plane, as shown in [10]. The electromechanical system also allows to predict the value of the stiffness achievable by the induced current forces, so that it can be verified that a specific magnetic suspension corresponds to desired specifications.
In this paper, the electromechanical model is applied on a homopolar null-flux electrodynamic bearing [4]. The identification of the model's parameters is done based on quasi-static FEM simulation results. Thanks to the insight the electromechanical model gives on the physics involved in the bearing, the dynamical stability and the stiffness of the bearing are analyzed as a function of the bearing spin speed. Afterwards, for various operation conditions like a constant external load, a static unbalance and different rotor weights, the behavior of the electrodynamic bearing is simulated and examined using the electromechanical model. For all these operation conditions, the influence of the external damping, necessary to stabilize the system is analyzed. The way to introduce this external damping, the amount of necessary damping is discussed and also its impact on the overall bearing consumption.

2 Electromechanical Model

The electromechanical model we will use throughout this paper is presented in [9], [10], [13] and [11] and is briefly reminded in this section. Its principle is to model the electromagnetic forces acting within a magnetic bearing by mechanical components like springs and dampers. Indeed, on the one hand, the reluctance forces and the forces between permanent magnets can be modeled by a stiffness k, when they are linearized by proportional to the relative displacement force. On the other hand, the Lorentz forces due to the interaction between induced currents, due to relative speed, and magnetic fields, can be modeled by introducing damping into the equations. Depending on following which kind of motion generates these eddy currents, they are modeled by rotating damping c_r or by non-rotating damping c_{nr}.
However, Lorentz forces resulting from the rotor spin motion can not be modeled by a simple constant rotating damping coefficient. Actually, when an electromotive force is induced on a conducting piece, the generated currents are subjected to inductive and resistive effects. Since the amplitude and the direction of the Lorentz forces depend on these induced currents, these forces are also subjected to these resistive and inductive effects.
These effects will be felt on the orientation of the force and on the norm of the force.
The model is based on the following considerations:

- the spinning speed ω is constant;
- there is no unbalance;
- relative displacements remain small, which means that the amplitude of the magnetic flux seen by the conductor $\left|\bar{\Psi}_0\right|$ can be assumed to be proportional to the amplitude of the center shift $|\bar{z}_I|$ through:

$$\left|\bar{\Psi}_0\right| = c_m \left|\bar{z}_I\right|$$

;

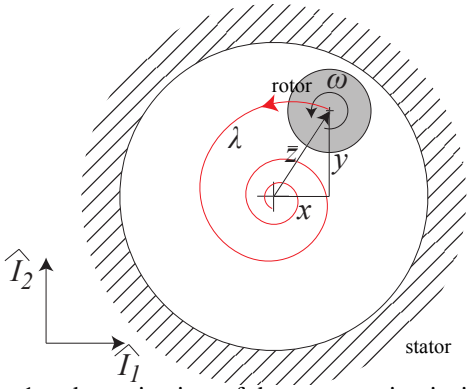

Figure 1: schematic view of the rotor motion inside the stator

- the electromagnetic variables vary in a way that may be approximated by a sinusoidal behavior;
- there are only eddy currents resulting from the rotor spinning motion;
- the resistive and inductive effects taking place in the conductor can be represented by a global resistance R_r and inductance L_r respectively.

The equation of motion characterizing a rotor of a magnetic bearing submitted to eddy current forces is:

$$\begin{aligned} m\ddot{\bar{z}}_I + (c_{nr} + c_r\cos\theta + jc_r\sin\theta)\,\dot{\bar{z}}_I + \\ (k + c_r\omega\sin\theta - jc_r\omega\cos\theta)\,\bar{z}_I = 0 \end{aligned} \tag{1}$$

where the position $(x_I; y_I)$ of the rotor in the plane perpendicular to the rotation is expressed by a complex vector $\bar{z}_I = x_I + jy_I$, and where ω is the rotor spin speed as illustrated in Fig. 1. It can be observed that cross-coupled terms are present in the stiffness and in the damping forces. Furthermore, in the stiffness force, we observe an induced stiffness, created by the spin speed and a component of the eddy current force, which is worth $c_r\omega\sin\theta$. The consequences of the resistive and inductive effects of the conductor experiencing the variation of flux appear in the expression of c_r and θ, expressed as:

$$\theta = \arctan\left(\frac{(\omega - \lambda_{Im})\,L_r}{R_r}\right). \tag{2}$$

$$c_r = \frac{c_m^2}{\sqrt{R_r^2 + ((\omega - \lambda_{Im})\,L_r)^2}}. \tag{3}$$

The global resistance R_r, the global inductance L_r and the constant proportionality factor c_m are parameters of the model specific to each magnetic bearing.

2.1 Advanced electromechanical model

Magnetic bearings are susceptible to work with a broad frequency spectrum and pass gradually from a situation where the skin effect is negligible to a situation where it becomes predominant. When the skin effect is negligible, at low frequency, the resistance and inductance are considered to be independent from the frequency, and at high frequencies the frequency evolution of the resistance and the inductance is generally well-known.
For the above presented electromechanical model, where the resistive and inductive effects of the conductors are represented by a resistance and an inductance, is thus important to have at our disposal a model of the variation of these latter with respect to the excitation frequency. The model we use has been presented in [12]. It is based on the continued fraction expansion of tanh function, and can be written as:

$$\bar{Z}(\omega) = R_{dc} + j\omega_{elec}L_0 + \cfrac{1}{\cfrac{3}{j\omega_{elec}L} + \cfrac{1}{\frac{5}{G} + \cfrac{1}{7j\omega_{elec}L + \ldots}}} \tag{4}$$

This model is based on four parameters: R_{dc}, L_0, G and L.

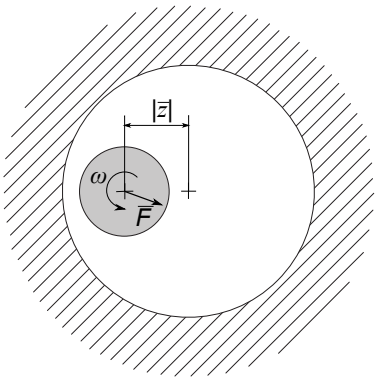

Figure 2: Configuration to identify the rotating damping $c_r(\omega)$

2.2 Parameter identification

The complete electromechanical model described through (1), the equations of motion, but also (2), (3) and (4) involves seven parameters. These different parameters are the stiffness k, the non-rotating damping coefficient c_{nr}, the proportionality constant c_m, the global inductance L_r, and the global resistance R_r for the rotating damping. The global inductance and resistance are characterized by four parameters: R_{dc}, L_0, G and L. When quantitative predictions are desired for a particular magnetic bearing, as it is the case in this paper, these parameters need to be identified. This identification can be done on the basis of force measurements, obtained through numerical simulations with finite elements or through experimental measurements.

As the practical case we will examine in the next section is an homopolar electrodynamic magnetic bearing, the parameters which will be needed to be identified are the parameters characterizing the rotating damping: c_m, L_r and R_r. To identify these latter, we can fix the spinning rotor in an out-centered position, and note down the values of the forces for different spin speeds (see Fig. 2).

In this particular configuration, the forces predicted by the model, when splitting between the restoring force in the direction of the center shift $\bar{z}$, called $F_{//}$ in the text, and the force in the direction perpendicular to the center shift, called $F_{\perp}$, are:

$$F_{//} = \frac{c_m^2 \omega^2 L_r}{R_r^2 + (\omega L_r)^2} |\bar{z}| \tag{5}$$

$$F_{\perp} = \frac{c_m^2 \omega R_r}{R_r^2 + (\omega L_r)^2} |\bar{z}| \tag{6}$$

It can be noticed that parameters are linked to each other by a scale effect. Only the ratios R_r/c_m^2 and L_r/c_m^2 can therefore be identified. This can be explained and understood by the fact that the R_r and L_r are the parameters of an equivalent circuit, excited by an electromotive force resulting from a flux variation. As there is a degree of freedom on the number of coil turns of this equivalent circuit, we choose to normalize by equaling c_m to 1.
Knowing the forces evolution for one off-centered position as a function of the spin speed, the identification of R_r and L_r is done by matching this evolution to the electromechanical model, with a least square criterion.

3 Practical case

The practical case presented here is an electrodynamical bearing (Fig. 3) developed by Lembke in [4] and commercialized by Magnetal AB. This electrodynamical bearing is based on a null flux scheme. Thanks to the homopolar design, no currents are induced until needed. In other words, currents are only induced when the rotor is out-centered. In this case, a fixed point on this rotating conductor will experiment a flux change, and currents are induced. These currents interact with the magnetic field and generate radial forces, as shown in Fig. 4. This means

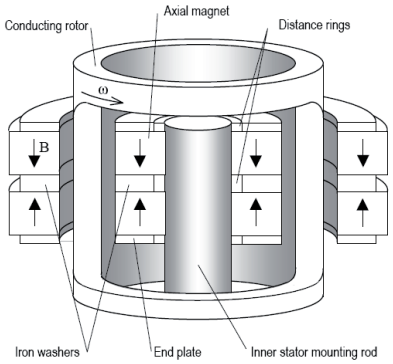

(a)

Figure 3: Homopolar radial electrodynamic bearing in [4]

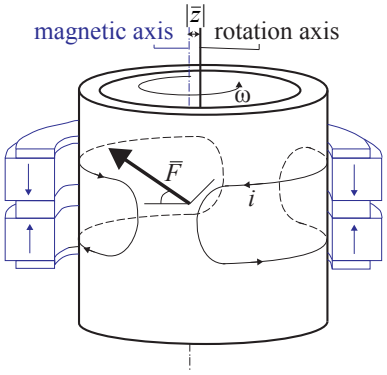

(b)

Figure 4: Principle of the electrodynamical bearing: resulting force from the interaction between the induced currents and the magnetic field when the rotor is out-centered

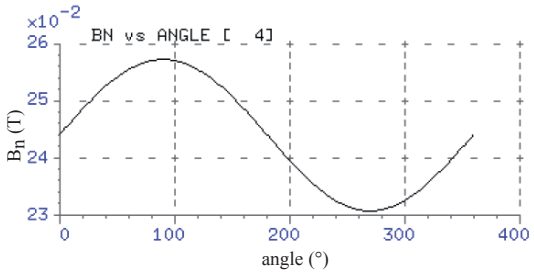

Figure 5: Norm of the magnetic induction along the rotor periphery, for $|\bar{z}| = 0.2$ mm, [4]

Table 1: Data of the electrodynamic bearing in [4]

OUTER MAGNET RING	
outer diameter/ inner diameter/ height	38 / 30 / 4 mm
remanent flux B_r	1 T
INNER MAGNET RING	
outer diameter/ inner diameter/ height	24 / 16 / 4 mm
remanent flux B_r	1 T
OUTER INTERMEDIATE WASHER	
outer diameter/ inner diameter/ height	38 / 30 / 2 mm
OUTER END PLATES	
outer diameter/ inner diameter/ height	38 / 30 / 1 mm
INNER INTERMEDIATE WASHER	
outer diameter/ inner diameter/ height	24 / 16 / 2 mm
INNER END PLATES	
outer diameter/ inner diameter/ height	24 / 16 / 1 mm
ROTATING COPPER CYLINDER	
outer diameter/ inner diameter/ height	29 / 25 / 9 mm
conductivity σ	60 10^6 $(\Omega m)^{-1}$

Table 2: Value of the parameters with and without skin effect identified on FEM forces

WITHOUT SKIN EFFECT	
$R = 0.1925\ \Omega$ $L = 4.41\ 10^{-5}$ H	relative residue on the error for the forces=0.39
WITH SKIN EFFECT	
$R_{dc} = 0.169\ \Omega$ $L_0 = 3.65\ 10^{-5}$ H $L_{cfe} = 3.49\ 10^{-5}$ H $G_{cfe} = 5.376$ S	relative residue on the error for the forces=$6.7\ 10^{-3}$

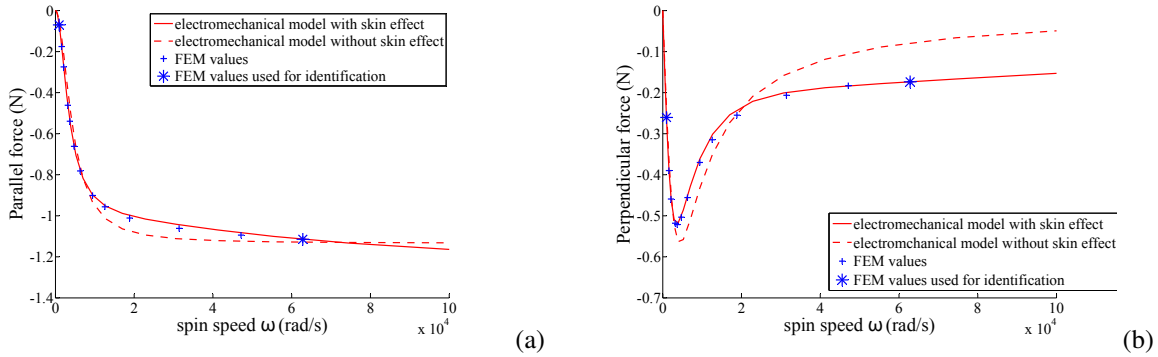

Figure 6: (a) Parallel and (b) Perpendicular forces as a function of the spin speed

that there is no stiffness, $k = 0$ and no non rotating damping $c_{nr} = 0$ generated by the electrodynamic bearing. The only parameters which need to be identified are the parameters characterizing the rotating damping parameter c_r.

FEM simulations, obtained from [4], give the parallel and the perpendicular forces value for different spin speed in a fixed out-centered position. In Fig. 5, the computed magnetic field for one given spin speed seen by a point rotating with the conductor is illustrated, and we see that the excitation is sinusoidal, as supposed. In this configuration, the forces are then worth (5) and (6). Their evolution with the spin speed is illustrated on Fig. 6, for a bearing whose dimensions are recapitulated in Table 1, and an eccentricity of $50\mu m$, that is 10% of the air gap. Based on these forces data, identification can be done considering the resistance R_r and inductance L_r as constants, i.e. without skin effect, or depending on the spin speed as predicted by (4), i.e. with skin effect. The value of the identified parameters are given in Table 2. The result on the predicted forces evolution with the spin speed and the comparison with the FEM calculated forces is shown in Fig. 6. Clearly, the model fits better when taking the skin effect into account. And this has an impact on the extrapolation of the forces at higher spin speeds, where the skin effect is more important.

Fig. 7 shows the evolution of the global rotor resistance and inductance when taking the skin effect into account or not.

With these identified parameters, let us now observe the induced stiffness $c_r\omega\sin\theta$ in Fig. 8. The induced stiffness stays quite low for low spin speeds, which shows the need to insert launch bearings in the system. The induced stiffness is directly linked to the spin speed ω, to the rotating damping coefficient, given by (3), and to the orientation of the force θ, given by (2). When introducing (2) and (3) in the expression of the induced stiffness $c_r\omega\sin\theta$, we obtain:

$$c_r \quad \omega \quad \sin\theta = \qquad (7)$$
$$\frac{c_m^2}{|z_I|^2\sqrt{R_r^2+((\omega-\lambda_{Im})L_r)^2}} \quad \omega \quad \frac{(\omega-\lambda_{Im})L_r}{\sqrt{R_r^2+((\omega-\lambda_{Im})L_r)^2}}.$$

It is interesting to note that, for a high spin speed, such as $\omega >> \lambda_{Im}$ and $\omega L_r >> R_r$, (7) tends to a constant value. Indeed, a first effect predominates when the reactance is much smaller than the resistance $R_r >> \omega L_r$, the induced stiffness increases with the spin speed because the norm of the induced currents do not depend on the spin speed, there is a n *omega* in the expression of the induced stiffness and the angle θ grows. But when the reactance is

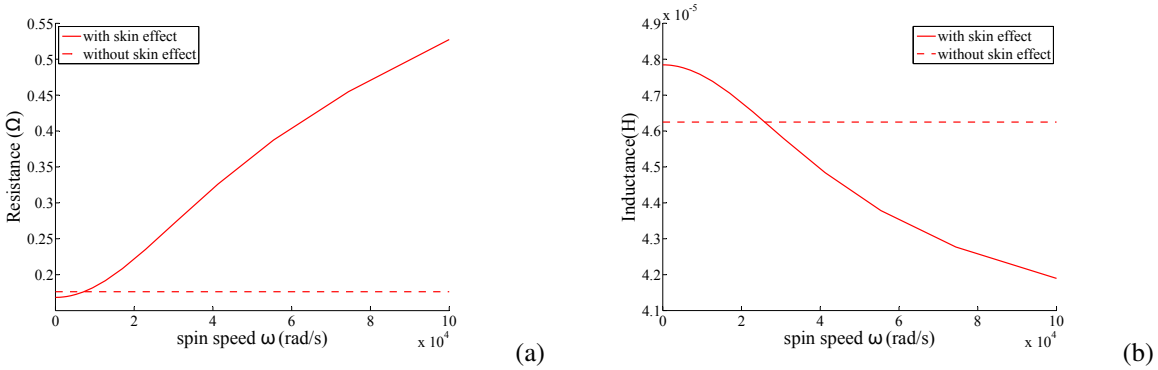

Figure 7: (a) Resistance and (b) Inductance as a function of the spin speed

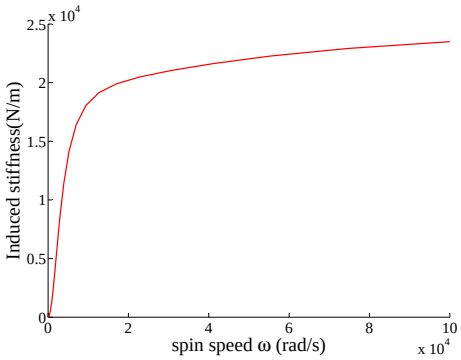

Figure 8: Induced stiffness $c_r \omega \sin\theta$

higher than the resistance, this effect is counteracted by the fact that the norm of the induced currents decreases with the spin speed, and the sinus term $\sin\theta$ tends to one. When $\omega L_r >> R_r$, in (7), the induced stiffness tends to a constant value.

4 Stability analysis

The aim of this paper is to show how the electromechanical model we developed is able to determine and explain the dynamical behavior and performances of an electrodynamic magnetic bearing, once its parameters have been identified properly. Indeed, as it will be explained in this section, the electromechanical system (1) shows the existence of an unstable spin speed range, or in other words the existence of two limit spin speeds between which the system behaves unstable in the radial plane. Above the second limit spin speed, the system is always stable. For appropriate values of the parameters, the rotor is always stable. In this section, based on the presented electromechanical model, the stability of a simple Jeffcott rotor supported by magnetic bearings is analyzed. The influence of the different parameters of the electromechanical model on the unstable speed range and on the induced stiffness is examined.

The system stability, based on (1), is studied by working in the Laplace domain, as explained in [10] and [11]. Using the Routh-Hurwith criterion, when (8) is negative, the system is unstable:

$$\begin{aligned} d_1 c_1 \quad = \quad & \left(c_{nr}^2 + c_r^2 + c_{nr} c_r \cos\theta\right) \\ & \left(-\frac{2c_r^2 m \cos^2\theta}{c_{nr} + c_r \cos\theta}\omega^2 + 2c_{nr} c_r \sin\theta\,\omega + 2k\left(c_{nr} + c_r \cos\theta\right)\right) \end{aligned} \tag{8}$$

It has to be noticed that in this equation, θ and c_r depend in a non-linear way on ω (see (2) and (3)), but also on λ_{Im}, the rotor whirl frequency, which is the solution of the equation of motion, which prevents an analytical

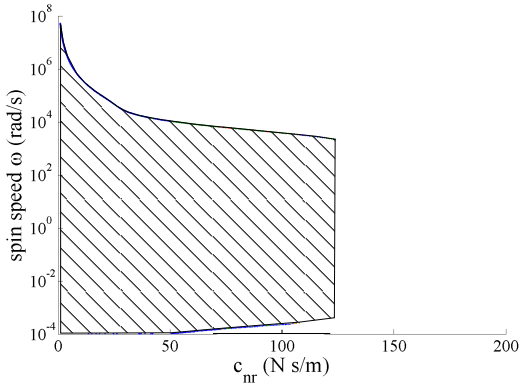

Figure 9: Evolution of the limit spin speed with the non rotating damping coefficient

solution. The solutions of (8), found numerically, show the existence of a limited speed range where the behavior of the system is unstable. Indeed, the spin speed can pass through a region where the system is unstable, and afterward reach a region where the behavior is stable.

We will now analyze the influence of the model parameters, like the non-rotating damping c_{nr}, the rotor weight m and the external stiffness k, on the stability.

For this analysis, we start from the different rotating damping parameters identified for the electrodynamical bearing [4] and summarized in Table 2. We fix the non rotating damping c_{nr} at 100 Ns/m. The mass of the electrodynamic bearing and the rotor m is fixed at 1 kg. Finally, we suppose there is no external stiffness ($k = 0$). This is the case when the electrodynamical bearing is used alone, when no other bearing introduces a radial stiffness. There are only centering forces due to induced currents.

4.1 Non rotating damping

Fig. 9 shows the evolution of the instability speed range according to the non rotating damping. For a system where the non-rotating damping is zero, the system is always unstable. On the other extreme, when the non-rotating damping is high enough, the system is always stable. Between these two extremes, there is a range of unstable spin speeds which decreases when the non rotating damping increases. We can notice, however, that the first limit spin speed for each non rotating damping has a very low value, and can be considered null. For the second limit spin speed, it decreases when the non-rotating damping increases, but it stays at high values.
In practice, introducing non rotating damping in the system is not easy to realize, since this damping has to be provided without contact between the stator and the rotor. One practical solution consists in inducing currents when the rotor whirls, but not when it spins, for example by mounting an homopolar permanent magnet on the rotor in front of a conductive part on the stator. This means mounting permanent magnets on the rotor, which spins very fast! Another solution could be to act externally on the stator which is not spinning, by placing a damper-spring between the stator and the ground for instance. This solution has been examined in [13] and [8].
At the same time, a pure viscous constant non-rotating damper has no influence on the induced stiffness value. This decoupling may be positive because it means that we can act on the stability thanks to this parameter without influencing the induced stiffness.

4.2 Mass

The instability speed range as a function of the system mass m is presented in Fig. 10. Below a certain value of m, there is no unstable spin speed. However, physically, m will have a minimal value, the bearing has its proper mass and has to carry a certain load.
The system mass has no influence on the induced stiffness value.

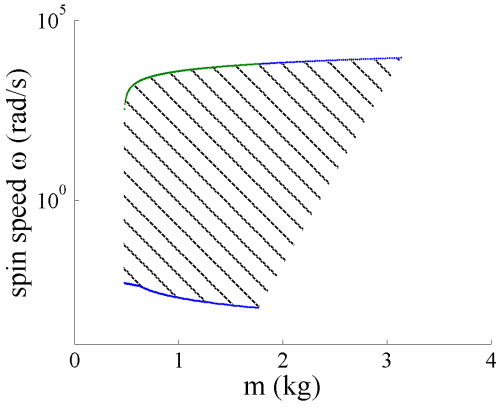

Figure 10: Evolution of the limit spin speed with the rotor weight

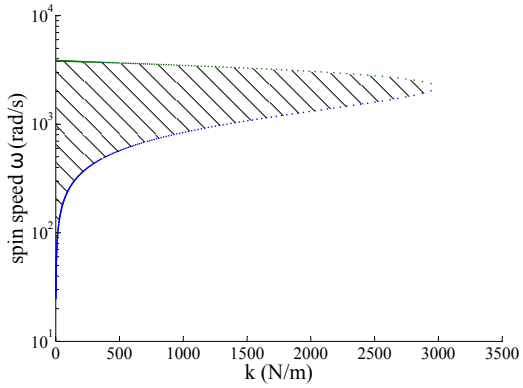

Figure 11: Evolution of the limit spin speed with the external stiffness

4.3 Stiffness

To complete this study, let us look at the impact of adding an external stiffness k to the system. Fig. 11 shows that it has a positive impact on the stability since the spin speed range where the rotor is unstable decreases with the stiffness, to vanish beyond a threshold value. We can see that adding an external stiffness to the system lowers the second limit spin speed, but mainly increases the first limit spin speed. When in the previous studies, we considered the first limit spin speed to be null, when adding external stiffness, this will not be the case anymore.
However, electrodynamic bearings are usually used in addition to a passive magnetic bearing, which then creates an external radial and axial stiffness, one being negative. With a negative radial stiffness, the upper limit spin speed, which allows a come back to stability, continues to increase.
Let us finally notice that the external stiffness has no influence on the induced stiffness value.

5 Power consumption

As electrodynamic bearings are fully passive devices, one might think that it is an interesting bearing to use in applications where the power consumption of the bearing has to be minimized. To have an estimation of the power consumption of the here above presented bearing, our electromechanical model can be used to realize a power balance, following this equation:

$$\sum P_{inj} = \sum P_{dis} + \frac{dW_{cin}}{dt} + \frac{dW_{pot}}{dt}, \tag{9}$$

where $\sum P_{inj}$ represents the power injected into the system, that it is to say, the power consumption of the system, $\sum P_{dis}$ represents the power dissipated into the dampers of the system, $\frac{dW_{cin}}{dt}$ represents the variation of kinetic energy inside the system and $\frac{dW_{pot}}{dt}$ represents the variation of potential energy inside the system.

Concerning the kinetic energy inside the system, it can be written:

$$W_{cin} = \frac{m(\dot{\bar{z}}_I \dot{\bar{z}}_I^*)}{2},$$

and from there on the variation of kinetic energy becomes:

$$\begin{aligned} \frac{dW_{cin}}{dt} &= \frac{1}{2}(m\ddot{\bar{z}}_I \dot{\bar{z}}_I^* + m\ddot{\bar{z}}_I^* \dot{\bar{z}}_I) \\ &= \frac{1}{2}(\bar{F}_I \dot{\bar{z}}_I^* + \bar{F}_I^* \dot{\bar{z}}_I) \\ &= \Re(\bar{F}_I \dot{\bar{z}}_I^*). \end{aligned} \tag{10}$$

According to (1), the forces in the inertial frame can be expressed as

$$\bar{F}_I = -(c_{nr} + c_r \cos\theta + j c_r \sin\theta)\dot{\bar{z}}_I - (k + c_r \omega \sin\theta - j c_r \omega \cos\theta)\bar{z}_I,$$

and (10) becomes

$$\begin{aligned} \frac{dW_{cin}}{dt} &= \Re(-(c_{nr} + c_r \cos\theta + j c_r \sin\theta)|\dot{\bar{z}}_I| - (k + c_r \omega \sin\theta - j c_r \omega \cos\theta)\bar{z}_I \dot{\bar{z}}_I^*) \\ &= -(c_{nr} + c_r \cos\theta)|\dot{\bar{z}}_I| - (k + c_r \omega \sin\theta)\,\Re(\bar{z}_I \dot{\bar{z}}_I^*) - c_r \omega \cos\theta\,\Im(\bar{z}_I \dot{\bar{z}}_I^*). \end{aligned} \tag{11}$$

The potential energy of the system is

$$W_{pot} = \frac{k(\bar{z}_I \bar{z}_I^*)}{2},$$

which means that the variation of the potential energy inside the system, it can be written:

$$\begin{aligned} \frac{dW_{pot}}{dt} &= \frac{k}{2}(\dot{\bar{z}}_I \bar{z}_I^* + \bar{z}_I^* \dot{\bar{z}}_I) \\ &= k\Re(\bar{z}_I \dot{\bar{z}}_I^*). \end{aligned} \tag{12}$$

Finally, the power dissipated into the dampers of the system can be split into two parts: the power dissipated into the non-rotating damping, and the power dissipated into the rotating damping. First, the power dissipated into the non-rotating damper can be expressed as:

$$\begin{aligned} P_{dis,c_{nr}} &= \Re(\bar{F}_{I,c_{nr}} \dot{\bar{z}}_I^*) \\ &= c_{nr}|\dot{\bar{z}}_I|^2. \end{aligned} \tag{13}$$

Second, to calculate the power dissipated into the rotating damper, it is important to place ourselves on the rotor, rotating at spin speed ω. The forces, resulting from the rotating damper, and expressed in a frame rotating at spin speed ω, predicted by the electromechanical model are equal to:

$$\bar{F}_{X,c_r} = (c_r \cos\theta + j c_r \sin\theta)\dot{\bar{z}}_X \tag{14}$$

where $\bar{z}_X$ is the complex expression of the rotor coordinates in the rotating frame $\hat{\mathbf{X}}$. By applying the appropriate frame transformation, the rotor position in the inertial frame can be linked to the rotor position in the rotating frame through $\bar{z}_X = \bar{z}_I e^{-j\omega t}$. This means that the rotor speed is worth:

$$\dot{\bar{z}}_X = (\dot{\bar{z}}_I - j\omega \bar{z}_I)\, e^{-j\omega t} \tag{15}$$

The mechanical power dissipated by the rotating damping can now be expressed as:

$$\begin{aligned} P_{dis,c_r} &= \Re(\bar{F}_{X,c_r} \dot{\bar{z}}_X^*) \\ &= (c_r \cos\theta + j c_r \sin\theta)\dot{\bar{z}}_X \dot{\bar{z}}_X^* \end{aligned} \tag{16}$$

From (15) and (16), it can be seen that the mechanical power is worth:

$$\begin{aligned} P_{dis,c_r} &= \Re\Big((c_r\cos\theta + jc_r\sin\theta)\left(|\dot{\bar{z}}_I|^2 + j\omega\left(\dot{\bar{z}}_I\bar{z}_I^* - \dot{\bar{z}}_I^*\bar{z}_I\right) + \omega^2|\bar{z}_I|^2\right)\Big) \\ &= c_r\cos\theta\,|\dot{\bar{z}}_I|^2 + c_r\cos\theta\,\omega^2|\bar{z}_I|^2 + c_r\omega\cos\theta\;\Im(\dot{\bar{z}}_I^*\bar{z}_I) \end{aligned} \tag{17}$$

Finally, replacing (11), (12), (13) and (17) into (9) leads to an expression for the power injected in the system:

$$\sum P_{inj} = -c_r\omega\sin\theta\Re(\bar{z}_I\dot{\bar{z}}_I^*) + c_r\cos\theta\,\omega^2|\bar{z}_I|^2 \tag{18}$$

The power injected into the system, in steady state, only depends on the rotating damping parameters. Or in other words, the power injected into the system, to maintain the rotor spinning at spin speed ω, is completely dissipated in the rotating damper.

6 Dynamical behavior

Previous developed equations of motion (1) of the parameterized electromechanical model considered that the rotor was a simple Jeffcott rotor with a constant spin speed, which is an oversimplification of the real world. In reality, the center of mass will not coincide with the geometric center, the rotor will not be a point mass, but will have moments of inertia. When rotating at very high spin speed, the flexural modes of the rotor might have to be taken into account, and so on. But even for more complex systems, the electromechanical model is an useful tool to predict the damping and the stiffness developed by the forces due to the induced currents at each moment. This damping and stiffness terms need then to be introduced into the mechanical equation governing the system, according to the hypothesis that are then considered: point mass rotor or not, perfectly balanced or not, small displacements or not...

6.1 Constant external load

In this section we will examine, through simulations, the behavior of the previously identified electrodynamic bearing when submitted to a constant external load of 5 H. The induced stiffness developped by this bearing has been examined on fig. 8. There is a non-rotating damper in the system to stabilize the bearing, and its value is 140 Ns/m, which means that without any external force, the rotor behaves stable for every spin speed. The rotor is perfectly balanced and its weight is 1 kg. The behavior of the rotor is illustrated in fig. 12. In fig. 12 (a), we see that the rotor does not spin fast enough ($\omega = 500$ rad/s) to induce enough stiffness in order to counteract the external load. But in fig. 12 (b), the rotor spins fast enough ($\omega = 2000$ rad/s) and the rotor reaches an out-centered equilibrium position.

The consumption of the bearing as a function of the spin speed is illustrated in fig.13. For low spin speed, the induced stiffness is not high enough, the rotor does not find an equilibrium position, which means a higher consumption. Once the value of the induced stiffness high enough to stabilize the rotor, the power consumption increases with the spin speed.

6.2 Unbalanced rotor

In the real world, the center of mass will never exactly coincide with the geometric center of the cross section of the shaft. The presence of this eccentricity ε will cause a static unbalance $m\varepsilon$. Supposing that the spin speed ω is constant, this unbalance generates a synchronous excitation . Then the motion of the geometric center will consist on the superimposition of the free motion, solution of the homogeneous differential equation (1), and a circular motion with an angular speed ω, particular solution of the differential equation. This means that the stability of the unbalanced system depends on the stability of the solution for free whirling. When this latter leads to a stable behavior, the unbalanced system is stable, but when it leads to an unstable behavior, this behavior will occur even if perfectly centered and without exterior disturbance because the unbalance will create the excitation. This is illustrated in fig. 14, with a non-rotating damping of 100 Ns/m. This shows the importance of having a correct dynamic model to be able to predict the dynamic performances of the whirling rotor in the useful speed range.

Regarding to the consumption of the bearing, when spinning at 400 rad/s and when modifying only the amount of non-rotating damping present, we can see in fig. 15 that, once the non-rotating damping is high enough to

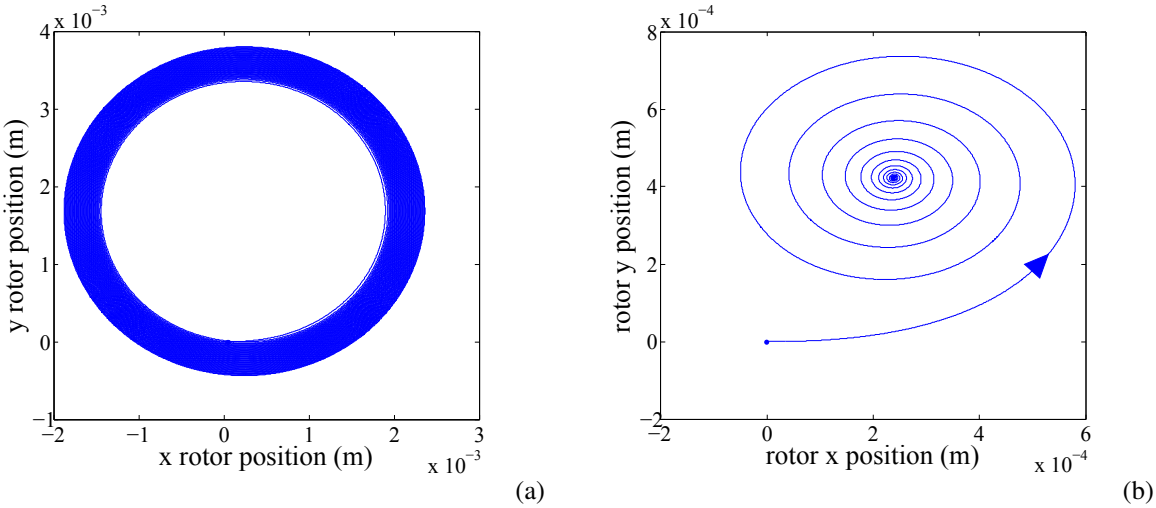

Figure 12: Rotor motion in the xy radial plane for a spin speed ω of (a) 500 rad/s: the rotor is unstable, (b) 2000 rad/s: the rotor is stable

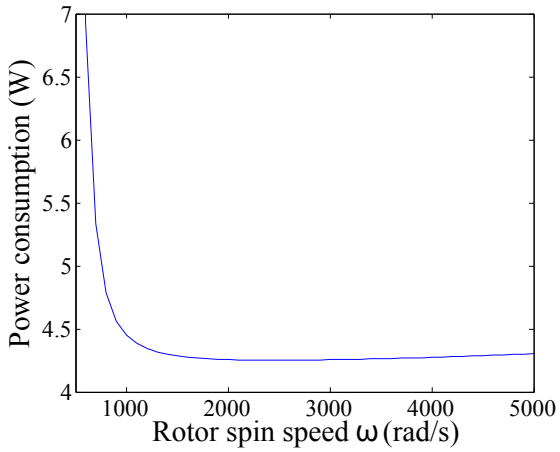

Figure 13: Power consumption of the bearing as a function of the spin speed, when submitted to a constant external load

stabilize the system, an increase of the non-rotating damping leads to a increase of the power consumption. For a non-rotating damping of 200 Ns/m, the instantaneous power is shown in fig. 16. This shows the repartition of the consumption in the stator, which is in this case in the non-rotating damping, and in the rotor, or in other words in the rotating damping.

7 Conclusion

The work presented in this paper develops how a parameterized electromechanical model which allows modeling the dynamical radial behavior of rotating electromagnetic systems submitted to induced current forces can be used to predict the dynamical behavior of a particular electrodynamical bearing and its consumption. We have shown that the model predicts unstable speed range. The model also predicts that the induced stiffness produced by eddy currents in the rotor is a function of the spin speed. Therefore, when working with electrodynamic bearings, attention has to be paid on those both aspects: instability and stiffness.

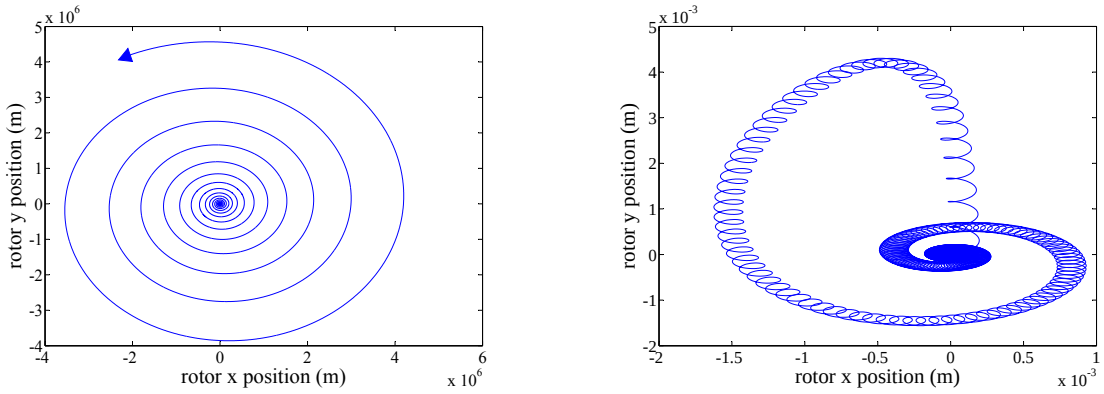

(a) (b)

Figure 14: Rotor motion in the xy radial plane for a spin speed ω of (a) 1000 rad/s: the rotor is unstable, (b) 10000 rad/s: the rotor is stable

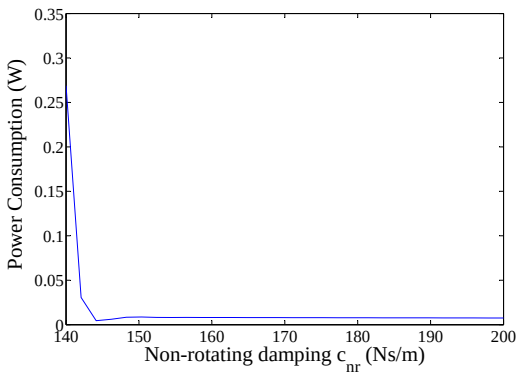

Figure 15: Power consumption of the bearing as a function of the non-rotating damping

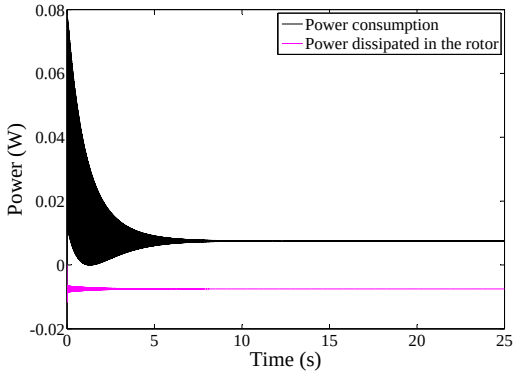

Figure 16: Instantaneous power consumption of the bearing, when spinning at $\omega = 400$ rad/s, and when the non-rotating damping is worth 200 Ns/m

References

[1] H. Bleuler, M. Cole, P. Keogh, R. Larsonneur, E. Maslen, R. Nordmann, Y. Okada, G. Schweitzer, and A. traxler. *Magnetib Bearings- Theory, design and Application to Rotaing Machinery*. Springer-Verlag, 2009.

[2] Earnshaw. On the nature of molecular forces wich regulate the constitution of the luminferous ether. *Trans. Cambridge Phil. Soc.*, 7:97–112, 1842.

[3] K. Davey, A. Filatov, and R. Thompson. Design and analysis of homopolar null flux bearings. *IEEE Transactions on Magnetics*, 41:1169–1175, 2005.

[4] T. Lembke. Design and analysis of a novel low loss homopolar electrodynamic bearing. Master's thesis, Royal Institute of Technology, Sweden, 2005.

[5] A. Filatov. Null-e magnetic bearings. Master's thesis, University of Virginia, USA, 2002.

[6] N. Amati, X. D. Lepine, and A. Tonoli. Modeling of electrodynamic bearings. *Journal of Vibrations and Acoustics*, 130(6), 2008.

[7] J.G. Detoni, F Impinna, N. Amati, and A. Tonoli. Unified modelling of passive homopolar and heteropolar electrodynamic bearings. *Journal of Sound and Vibrations*, 2012.

[8] A. Tonoli, N. Amati, F. Impinna, and J.G. Detoni. A solution for the stabilization of electrodynamic bearings. *Journal of Vibrations and Acoustics*, 133(2), 2011.

[9] V. Kluyskens, B. Dehez, and H. Ben Ahmed. Dynamical electromechanical model for magnetic bearings. *IEEE Transactions on Magnetics*, 43(7):3287–3292, 2007.

[10] V. Kluyskens and B. Dehez. Parameterized electromechanical model for magnetic bearings with induced currents. *Journal of System Design and Dynamics*, 3(4):453–461, 2009.

[11] V. Kluyskens and B. Dehez. Dynamical electromechanical model for magnetic bearings subject to eddy currents. Submitted.

[12] V. Kluyskens and B. Dehez. Comparison between models predicting the evolution of the electrical impedance with frequency. *International Journal of Circuit Theory and Applications*, 39:973–982, 2011.

[13] V. Kluyskens. Dynamical electromechanical model of magnetic bearings subject to eddy currents. Master's thesis, Universite Catholique de Louvain, Louvain-la-Neuve, Belgium, 2011.

8 Acknowledgment

The electrodynamic bearing on which the analysis is made was developed by [4], and is commercialized by Magnetal AB.